Injection-molded Ceramics: Critical Aspects of the Binder Removal Process and Component Fabrication

G. Bandyopadhyay & K. W. French*

GTE Laboratories Inc., 40 Sylvan Road, Waltham, Massachusetts 02254, USA

Abstract

An injection-molding process for silicon nitride ceramics with a wax-based thermoplastic binder system is critically evaluated to determine the binder removal mechanisms and the role of the binder removal process on the cracking of components. Binder removal is described in terms of three mechanisms: binder loss due to melting and thermal expansion, wicking of liquid binder due to capillary pull from the setter bed, and binder volatilization. Burnout cracking could easily be eliminated from small cross-section (< 1 cm) parts with small volume to surface ratio (e.g. modulus of rupture (MOR) bars). However, variations of the wicking and volatilization environment by changes of setter bed and thermal cycle, including substantial slowing down of the cycles, could not eliminate cracking from large cross-section parts such as a radial turbine rotor. Significant changes in cracking pattern in rotors as a result of enhanced wicking indicated that wicking-induced particle rearrangement during binder burnout played a key role in component cracking.

Ein Druckgußverfahren zur Herstellung von Siliziumnitrid-Keramiken mit einem thermoplastischen Bindersystem auf Wachs-Basis wird kritisch beurteilt, um die Mechanismen der Entfernung der Binderphase und die Rolle dieses Entfernungsvorganges auf die Rißbildung von Komponenten zu bestimmen. Die Entfernung des Binders wird mittels dreier Mechanismen beschrieben: Binderverlust infolge von Aufschmelzen und thermischer Ausdehnung, Herausziehen des flüssigen Binders aus dem Pulverbett aufgrund kapillarer Kräfte und Abdampfen des Binders. Die Bildung von Rissen, die beim Brennen der Keramik entstehen können, konnte bei Teilen mit geringem Querschnitt (≤1 cm) und geringem Volumen zu Oberflächenverhältnis (z.B. bei MOR-Stäbchen) leicht vermieden werden. Bei Teilen mit großem Querschnitt, wie beispielsweise bei einem Radial-Turbinenrotor, konnten Risse aufgrund von Veränderungen der äußeren Bedingungen beim Herausziehen und Verdampfen des Binders, die auf ein verändertes Pulverbett und thermische Zyklen—das entscheidende Verlangsamen der Zyklen mit eingeschlossen—zurückzuführen sind, nicht eliminiert werden. Signifikante Veränderungen im Rißbild von Rotoren infolge verstärkten Herausziehens der Binderphase zeigten, daß die hierdurch herbeigeführte Umordnung der Teilchen beim Ausbrennen des Binders eine Schlüsselfunktion bei der Rißbildung von Komponenten einnimmt.

Cet article présente l'évaluation critique d'une technique de moulage par injection de céramiques en nitrure de silicium, utilisant un système de liants thermoplastiques à base de cires, afin de déterminer les mécanismes d'élimination des liants et le rôle du déliantage sur la fissuration des composants. Le déliantage est décrit sur base de trois mécanismes: la perte de liant due à la fusion et à la dilatation thermique, la succion capillaire du liant liquide dans le lit-support et la volatilisation. Les fissures engendrées par la combustion peuvent être facilement éliminées lorsque l'on traite des composants à faible section (< 1 cm) et à faible rapport volume sur surface (par exemple: des barres de mesure du module de rupture). Cependant, on ne peut pas éliminer les fissures lorsque l'on traite des composants à grande section, comme des turbines radiales de rotor, même en modifiant la succion capillaire et la volatilisation, en jouant sur les caractéristiques du lit et du cycle thermique, y compris par un traitement à beaucoup plus basse température. On remarque que le réarrangement des particles dû à l'augmentation de la succion capillaire durant le

*Consultant.

23

déliantage joue un rôle clé dans la fissuration des composants, comme l'indiquent les modifications significatives constatées sur les cartes de fissuration des rotors.

1 Introduction

In recent years, the injection-molding process has attracted considerable attention as a technique for the fabrication of complex net shape ceramic components such as automotive turbochargers and gas turbine vanes, blades and rotors.[1-7] The primary driving force for developing this technology for ceramics is to exploit the high-volume, cost-effective production capability of the injection-molding process for fabrication of net shape components, thereby eliminating or minimizing the expensive grinding cost associated with the machining of ceramic parts.

Injection molding of ceramics generally requires selection of an organic or aqueous binder system and normally consists of five steps: powder processing, compounding of the powder with the binder, injection molding, binder removal, and densification by sintering and/or hot isostatic pressing (HIPing). Control of each of these process steps and appropriate selection of the starting material (powder and binder) are critically important to the overall process success. Despite the large number of variables and the complex interrelationship among these variables, significant technical successes have been reported[4-11] by ceramic and engine manufacturers on the fabrication and performance (in the laboratory and in engine environments) of both small and large cross-section injection-molded silicon nitride and silicon carbide components for heat engine applications. The details of the component fabrication process, however, have largely remained proprietary and have not been reported in the open literature. It is, therefore, difficult to assess the state of the technology, specifically in relation to its potential for large-scale commercialization.

In recent years, a number of publications have addressed basic aspects of ceramics and metal injection molding including the various possible mechanisms of binder removal processes.[12-19] These studies are generally limited to model systems and simple geometries; however, they provided valuable guidelines for selecting preferred binder systems and burnout environment. Mechanistic descriptions of thermal binder removal processes included thermal expansion induced binder transport,[13] wicking controlled removal into a powder bed,[14,15,18-20] and thermal degradation of the organic binder in an inert or oxidizing environment.[13-17] Both capillarity-driven liquid transport

to the part surface followed by vaporization and diffusion controlled gas-phase transport have been shown to be important during binder removal from a ceramic part. In recent studies,[21-23] attempts have been made to relate cracking during burnout to starting powder particle size, particle rearrangement and resulting part shrinkage, as well as to the polymer removal stages. Cracking during binder removal, however, remains the overwhelming concern in fabrication of injection-molded ceramics specifically for complex, thick cross-section components such as a radial turbine rotor. This paper describes the results of an effort devoted to understanding the binder removal process and its influence on cracking behavior in both small (<1 cm) and large (>1 cm) cross-section injection-molded parts.

During the course of this investigation, a large number of silicon nitride parts of different geometries were injection molded using a wax-based thermoplastic binder system (described in Section 2.2).[24] For small cross-section components, cracking during binder burnout is a less serious issue; generally cracks can be eliminated by slowing down the thermal cycle and/or by using an inert environment that prevents disruptive exothermic reactions of binder with oxygen. High-quality sintered and HIPed components of both simple (modulus of rupture (MOR) bars) and airfoil (blades and vanes) geometries have been fabricated.[9,11,25] The large cross-section parts, however, are much more prone to cracking during the binder removal step.[7] The difficulty arises due to noniniform shrinkage that occurs during burnout; the nonuniformity cannot be eliminated by simply slowing down the thermal cycle or changing the burnout atmosphere.[20] In many cases, burnout-related flaws appear as inhomogeneities or defects too small to be detected after binder removal, but become visible only after the parts are sintered to high densities. Cracks can appear as internal laminations and/or surface connected external flaws. The nature and extent of cracking depends strongly on the powder characteristics, binder removal conditions and part geometry. Although a specific binder type was used in this investigation, the binder removal mechanisms and the cracking behavior described in this paper are believed to be appropriate for other similar thermoplastic binder systems, but may not apply where thermoset or partial thermoset binders are used.

Section 2 of this paper describes fabrication procedures for test samples and components. The role of some significant process variables, the binder removal mechanisms, and the results and implication of the binder removal experiments on cracking of components are discussed in Section 3. Finally, Section 4 summarizes the major conclusions.

2 Fabrication of Test Samples/Components

2.1 Powder processing: composition and characteristics

All test components (small and large cross-section) were fabricated from GTE SN502 (GTE Chemical and Metallurgical Division, Towanda, PA) silicon nitride powder containing 6 wt% yttria and 2 wt% alumina as sintering additives (referred to hereafter as AY6 composition). The SN502 was 99·99 wt% pure with respect to metallic cations and had <2 wt% oxygen as determined by inert gas fusion. The as-received powder was characterized as >95% α-phase silicon nitride with needle-shaped and equiaxed particles (Fig. 1), and had a BET surface area of approximately 4 m²/g. The yttria (Molycorp Grade 1600, White Plains, NY) and alumina (Reynolds Metal Co., Richmond, VA) powders were 99·99% pure with BET surface area of greater than 3 m²/g.

The silicon nitride with sintering additives was ball milled for subsequent processing. A series of experiments was performed to optimize the milling conditions to provide for easy and reproducible compounding and molding. Figure 2 shows the typical milled AY6 powder micrograph, which indicates that the SN502 needles were effectively broken up during the milling process to yield essentially equiaxed particle morphology. The BET surface area for typical milled powder was 9–13 m²/g, with a calculated mean particle size of 0·12–0·22 μm. X-Ray sedigraph measurements, however, showed a substantially larger mean particle size (1·36–2·20 μm) and size distribution (Fig. 3), indicating that the powder after milling exhibited a strong tendency towards agglomeration. The significance of agglomeration in ceramic processing is well known. In injection molding, the loose and soft agglomerates can generally be broken up[25,26] during the high shear compounding and molding
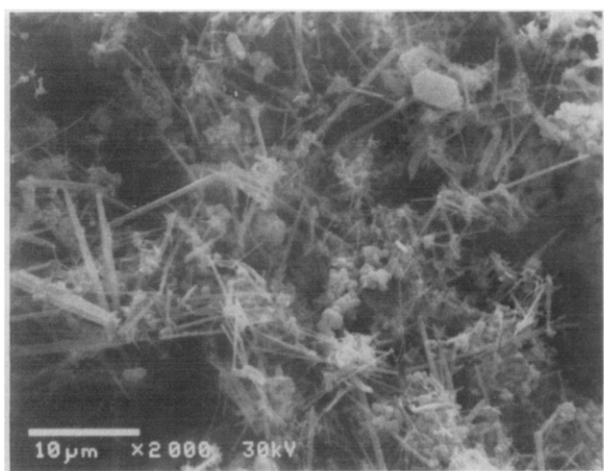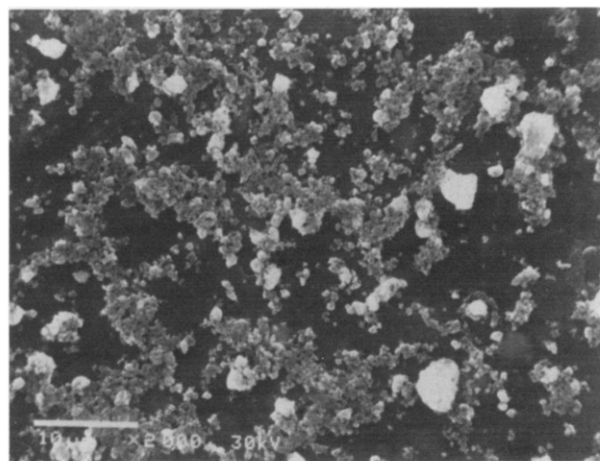

Fig. 2. Scanning electron micrograph of milled AY6 silicon nitride powder.

steps, and a highly uniform green microstructure can be obtained by this process. The hard agglomerates, however, may significantly impact on the compounding and molding step as well as the final material properties. The impact of the starting powder on subsequent processing will be described further in relation to the description of the compounding of the material.

2.2 Binder selection

The binder used in this study is a simple system containing 90 wt% paraffin wax (1865Q wax, Astor Chemical, Harrison, NY), 5 wt% epoxy thermosetting material (Acme 5144, Allied Products Corp., New Haven, CT) and 5 wt% surfactant (oleic acid A-215, Fisher, Medford, MA).[24] This system is thermoplastic in nature and has several characteristics which are highly desirable for fabrication of complex shaped parts. Some of the characteristics are: (a) a low softening range (40 to 80°C) to reduce the temperature gradient between injection barrel and mold—the gradient, in turn, minimizes the cooling-related shrinkage, thus preventing blade cracking in the mold; (b) a low viscosity, required for adequate melt flow at relatively high ceramic loadings; (c) a room-temperature flexibility which is

Fig. 1. Scanning electron micrograph of as-received GTE SN502 silicon nitride powder.
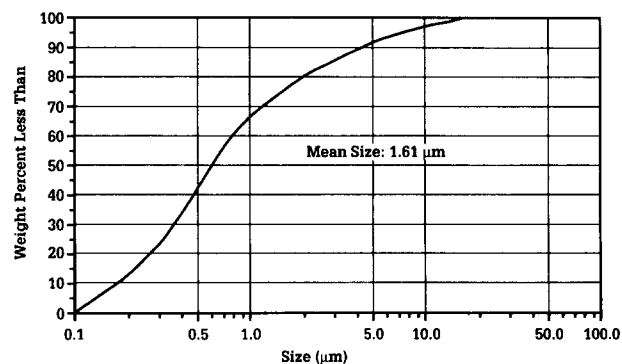

Fig. 3. Typical particle size distribution (by X-ray sedigraph) for milled AY6 silicon nitride powder.

imparted by the plasticizing effect of the liquid epoxy; and (d) ease and completeness of removal in a thermal binder removal cycle.

2.3 Compounding

The compounding step involved mixing of an appropriate weight fraction of milled AY6 powder with the organic binder at approximately 70°C to produce a mixture which behaves like a thermoplastic material capable of forming by the injection-molding process. A 1·6-liter Bramley mixer equipped with dispersing-type blades was used to compound the powder with the binder system. The powder was dried prior to compounding to eliminate moisture entrapment. Air entrapment was eliminated by slowly mixing the compounded material under vacuum and subsequent molding of the parts using evacuated molds.

The particle size, shape and size distribution of the starting powder are known to strongly influence the viscosity of the compounded mix and the moldability.[2,27-29] A convenient approach to determine moldability is to measure the flow distance in a spiral flow test mold[28,29] used under typical injection-molding conditions. It has been shown that[28]

$$d = A/\eta \qquad (1)$$

where d is the spiral flow distance, A is a constant, and η is the viscosity of the powder/binder mixture. η can further be expressed as

$$\eta = \eta_0(1 - V)^{-K} \qquad (2)$$

where η_0 is the viscosity of the binder, V is the volume powder loading, and K is a powder-dependent parameter.[27] K ranges from 21 for monomodal, 5·8 for bimodal and 3·6 for trimodal to 3 for infinite modal systems. Combining eqns (1) and (2), one gets

$$d = A/\eta_0(1 - V)^{-K} \qquad (3)$$

which provides a relationship between the spiral flow distance and the volume percent powder loading for a specific molding condition.

Spiral flow measurements were made in a transfer press with the compounded powder/binder system prepared from three different silicon nitride lots at four different powder loadings. The barrel temperature was maintained at 68–70°C, the mold temperature was 38–40°C, and a 51·7 MPa injection pressure in the cavity was used. Figure 4 shows the straight line relationship, as expected from eqn (3), when log d was plotted versus log $(1 - V)$ for the present series of experiments. Despite the use of different silicon nitride powder lots, the processed material showed similar flow characteristics, indicating the consistency of the rheological properties of the powder. A K value of 5·2 was obtained from the
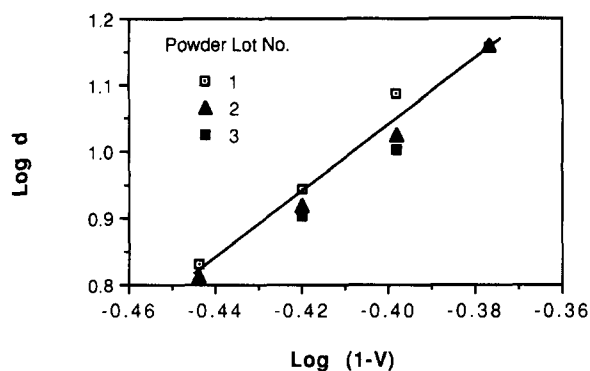

Fig. 4. Relationship between spiral flow distance (d) and vol.% powder loading (V) for the compounded AY6 silicon nitride powder/binder mix.

slope of the straight line, indicating that the particle size distribution in the compounded material is close to bimodal. Figure 5 shows the scanning electron micrograph of a typical compounded powder/binder mix. It is evident that the majority of the large agglomerates were broken up to basic particles during compounding. However, a small percentage of the large agglomerates remained in the compounded mix. Thus it can be assumed that the flow behavior in molding was determined by the primary particles as well as the remaining agglomerates.

2.4 Injection molding

The injection-molding step involved heating the mixture above its flow point and injecting it into a relatively cold mold where the material solidified, taking the shape of the mold. Any flaw (voids/cracks) or flaw precursor (e.g. in the form of residual stress) in the molded part cannot be eliminated during the subsequent binder removal and sintering process steps. Thus these problems must be eliminated from the molded part.

In the present investigation, molding of silicon nitride parts was accomplished in both plunger-type
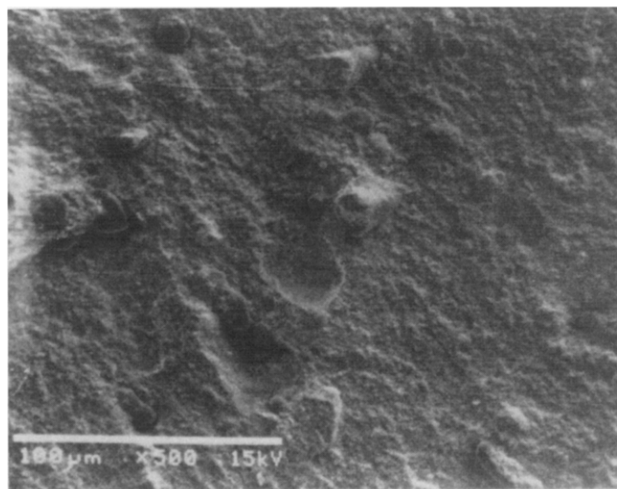

Fig. 5. Scanning electron micrograph of 62 vol.% compounded AY6 powder/binder mix showing the presence of a limited number of large agglomerated particles.

and reciprocating-screw-type injection-molding machines. The key parameters that need control during the molding step are mold and melt temperature (typically 35–40°C and 68–72°C, respectively) and cavity injection pressure (51·7–86·2 MPa). In general, optimization of these parameters is required for each component geometry in order to produce parts free from visual and X-ray detectable flaws. In addition to optimization of the molding variables, cavity evacuation and/or venting were sometimes required to eliminate undesirable fold lines and residual voids due to entrapped gas.

Many hundreds of small and large test parts were successfully molded for this study and related programs. The parts were free from visual and X-ray detectable defects, and exhibited excellent green microstructural homogeneity.[26] This characterization, however, did not address the general concerns on molding-related residual stresses which may introduce defects that become visible only after the binder removal process.[22,30] In the present study, surface and internal cracking patterns in densified parts were altered extensively and reproducibly by changing the binder removal parameters only. Molding variables, when controlled within the optimized values, had little effect in these experiments. Thus it is concluded that molding parameters did not influence the cracking behavior described in this paper. It should be pointed out, however, that lack of control in the molding step can indeed introduce gross cracking in the binder removal step.

2.5 Binder removal

The injection-molded parts are then subjected to the binder removal process. The complete and non-disruptive removal of the organic binder from the formed part is accomplished in this process step. To eliminate deformation and/or slumping at the early stages of binder removal, the parts are embedded in a sand or setter powder. The use of a setter bed for processing of injection-molded complex-shaped components is an important and sometimes necessary variable. Recently, some experiments and analyses with selected ceramics and metallic systems[14,15,18,19] on the impact of such powder bed on binder removal have been described in the literature. In addition to the part support, the setter powder type (specifically the powder particle morphology) may strongly influence the mechanism of liquid binder removal from the part surface to the setter bed and thus may influence the binder removal process. A high surface area powder bed is expected to create a strong capillary pull with an effective 'wicking power'. A low wicking setter bed, on the other hand, could encourage binder loss by vaporization by slowing down the wicking process. Two setter types representative of a high wicking (high

Table 1. Characterization of setter powders used for binder removal

Setter type	Composition	BET surface area (cm^2/g)	BET particle size (μm)
Fine	Chromatographic grade alumina[a]	68·40	0·02
Coarse	Calcined AY6 silicon nitride[b]	0·20	9·31

[a] Baker Reagent No. 1-0540, Boston, MA.
[b] Calcined at 1800°C or higher under N_2 pressure and screened through a 100-mesh screen.

surface area) behavior and a low wicking (low surface area) behavior were selected for this study based on evaluations of a number of inert powder materials such as alumina, silicon nitride, glass beads and charcoal. Table 1 summarizes the characteristics of the two selected setter materials. Chromatographic alumina was used as the high wicking, high surface area setter powder, referred to henceforth as the 'fine' setter, while calcined silicon nitride was used as the low wicking 'coarse' setter powder.

Binder removal was carried out in a nitrogen environment to eliminate disruptive exothermic reactions of binder with oxygen. The residual carbon was removed after the binder burnout by heating the part in air to temperatures up to 600°C. A wide variety of thermal cycles were used to study the rate and mechanism of binder loss from parts. The details of some of the key thermal cycles are described in Section 3.

2.6 Densification

Densification was primarily carried out by sintering at 1750°C or higher in a static overpressure of nitrogen. One of the key objectives of densification in this study was to reveal the internal and external cracks that could not be easily detected after the binder removal process.

3 Results and Discussion

3.1 Binder loss studies

The binder loss experiments in the present work were designed to understand the effects of part geometry and burnout setter on binder loss mechanisms and their impact on component cracking. A series of interrupted binder removal experiments were performed using injection-molded MOR bars (4·8 × 8·6 × 61·0 mm) and spheres (22·1 mm dia.) with 62 vol.% ceramic powder loading, and prototype configuration gas turbine rotors (Fig. 6) for the AGT 100 engine designed by Allison Gas Turbine Division of General Motors Corporation.[10] The rotor represented a complex engine part containing
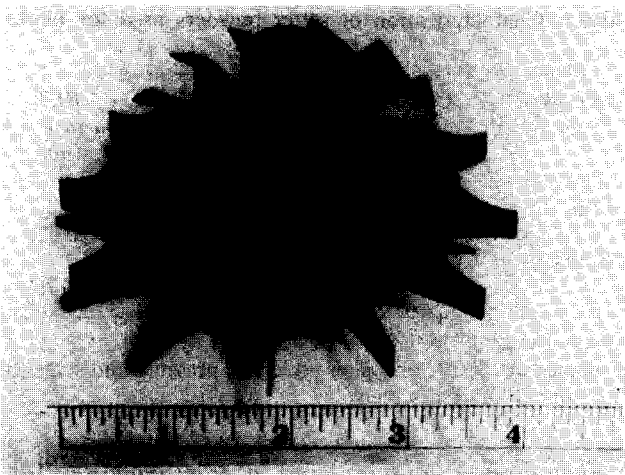
Fig. 6. Injection-molded silicon nitride AGT 100 gas turbine rotor.

(a)

(b)

(c)

Fig. 7. Binder loss data from interrupted burnout experiments (heating rate $10°C/h$) in (a) fine and (b) coarse setter. (c) TGA weight loss data at $12°C/h$ for the powder/binder system are also shown. □, MOR bar; ▲, sphere; ■, AGT 100 rotor.

thin and thick sections (maximum hub section in the as-molded condition was approximately 75 mm while the thinnest section at the blade tip was <1 mm). A powder loading of 60 vol.% was used for fabrication of these rotors. The test samples were buried in one of the two setters identified in Table 1. The typical thermal cycle used for these tests was a $10°C/h$ heating rate to $450°C$ in N_2. Samples were removed from the furnace at various stages of the thermal cycle, and their weights and dimensions were measured. In the case of rotors which were withdrawn at temperatures exceeding $290°C$, test samples were cooled at the natural rate of the furnace for approximately 1 h prior to their removal from the oven.

Figure 7 shows the binder loss data from the interrupted experiments as a function of burnout temperatures for the two setter types. For comparison, the weight loss data obtained by thermogravimetric analysis (TGA) in N_2 of the powder/binder mixture with no setter are also shown in Fig. 7. The TGA data represent vaporization in an open environment (absence of setter precludes wicking). In addition, since small amounts of powdered samples were used, weight loss in the TGA was not influenced by size or shape consideration.

The data in Fig. 7 show the effects of both part size and shape, and setter type. Not surprisingly, the binder loss occurred at higher temperatures for larger cross-section parts. The setter type also influenced the weight loss behavior significantly. However, despite the variations and the large weight loss, the overall dimensional shrinkages were insignificant in all test parts. Figure 8 shows the dimensional change data obtained from the interrupted tests on MOR bars and spheres. Although MOR bars showed slightly more shrinkage than the spheres, the absolute magnitude of the dimensional change was insignificant except for the small linear shrinkage (up to 1%) detected only when the
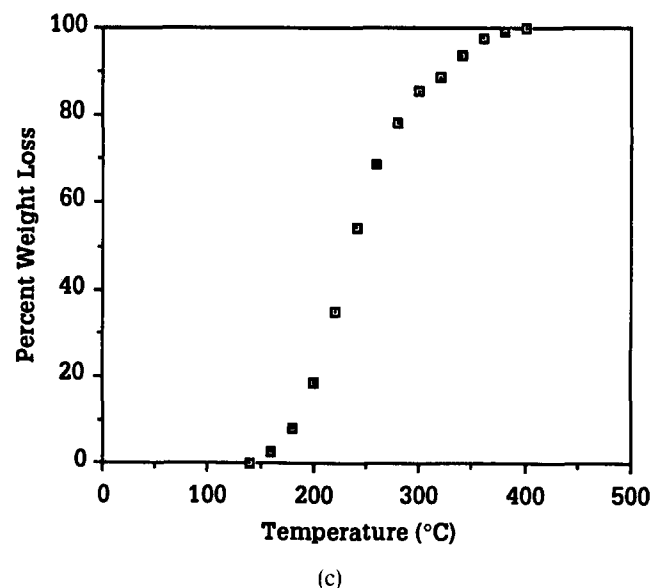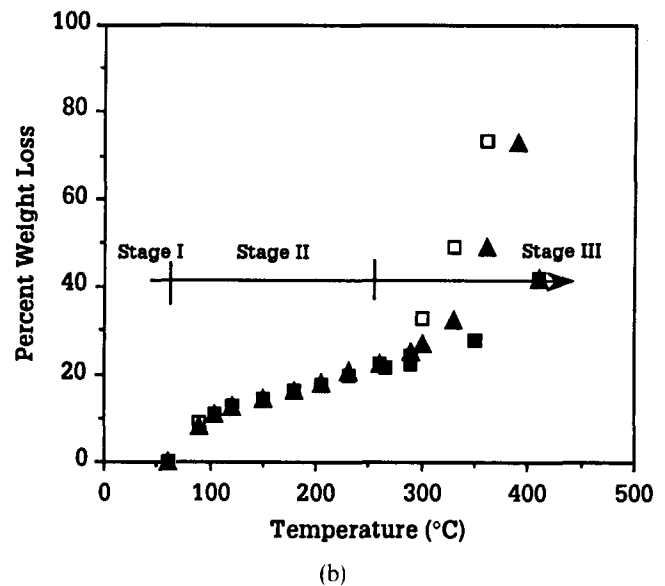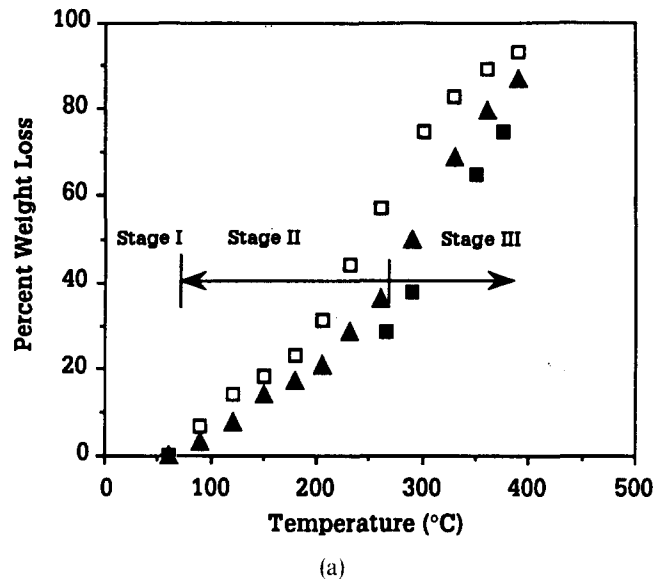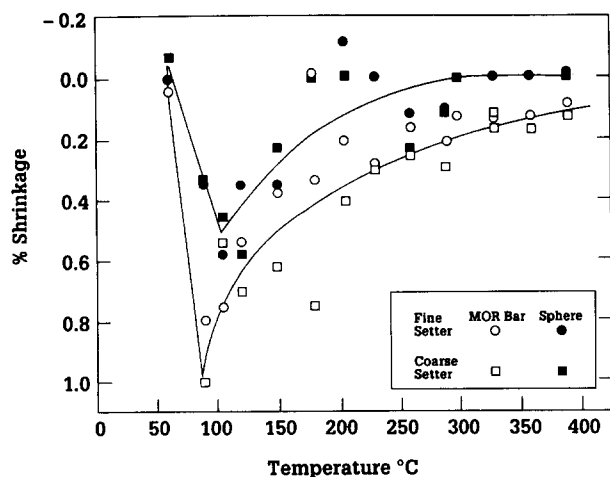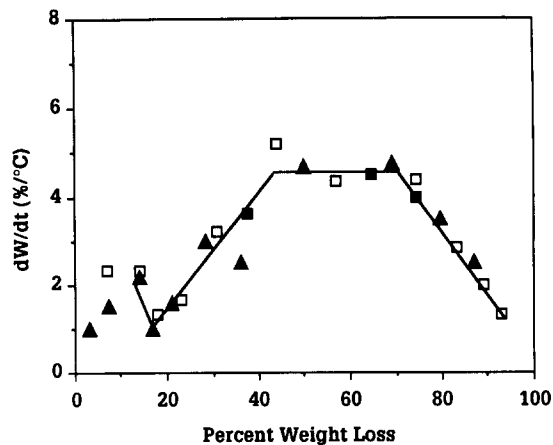
Fig. 8. Dimensional change data from interrupted burnout experiments.

(a)

(b)

Fig. 9. Relationship between rate of weight loss and percentage binder loss for different part geometries and cross-sections. □, MOR; ▲, sphere; ■, rotor. Binder removal thermal cycle 10°C/h. The data show a unique relationship for each setter type: (a) fine setter; (b) coarse setter.

burnout was interrupted between 90 and 120°C. These dimensional change results are in agreement with the real-time measurements, which revealed very minor volume change during burnout of MOR bars in an 'X-ray transparent oven'.[31] Dimensional measurements of AGT 100 rotors also showed very little shrinkage in burnout.

The weight loss behavior shown in Fig. 7 for the two setter types can broadly be divided into three stages (as shown in the figure). Stage I, as defined in this paper, represents the initial weight loss that started on melting of the binder at approximately 60°C. The wax/epoxy binder system showed 23% volume expansion on melting. Since none of this volume change was visually observed in the parts during binder removal (a part containing 40 vol.% binder should expand by approximately 9%), it is concluded that the expanding binder, as it melted, flowed out of the part into the setter.

The Stage I weight loss is similar to the initial transient stage described by Bao & Evans[19] in their studies on capillary extraction of organic vehicles from ceramic bodies. The existence of this initial stage is confirmed when the data from Fig. 7 are replotted in a form similar to drying rate curves (Fig. 9); this figure shows a change of mechanism (as indicated by the appearance of a minimum) for both setter types at approximately 18% binder loss. It appears that an excess amount of liquid binder becomes available in the surface at the initial stage as a result of expansion of the binder in a fully saturated compact. The drainage of liquid from the surface at this stage is influenced by gravity as well as by the pore morphology, particle size and wettability of the setter powder bed. This process of binder loss is expected to continue until mass removal from the surface by wicking or by surface evaporation becomes rate controlling.

The weight loss in Stage II is defined in this paper (approximate temperature range 100–280°C) as the
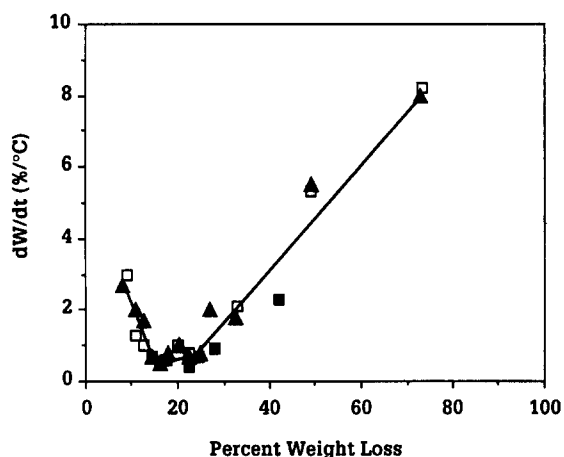
region in which the wicking power of the setter material determined the rate at which liquid binder was removed from the part surface to the setter powder. For example, binder loss continued at a relatively rapid pace (Figs 7 and 9) with the high surface area fine setter powder, whereas weight loss in the coarse setter slowed down significantly due to formation of a thick cake (which acted as a barrier) around the sample. The significance of the setter powder in Stage II of the process is further demonstrated in Fig. 10, where weight loss data from isothermal burnout experiments at 125 and 150°C (at which binder vaporization is expected to be minimal) on MOR bars are shown as a function of $t^{1/2}$ for both fine and coarse setters. In these experiments, the MOR bars were removed from the oven at fixed intervals (after the isothermal temperature was reached at 10°C/h) and their weights were measured. It is evident that binder loss could continue in fine setter due to the strong wicking forces, whereas the weight loss remained virtually unchanged with time in the coarse setter. Since wicking did not occur in the coarse setter, the par-
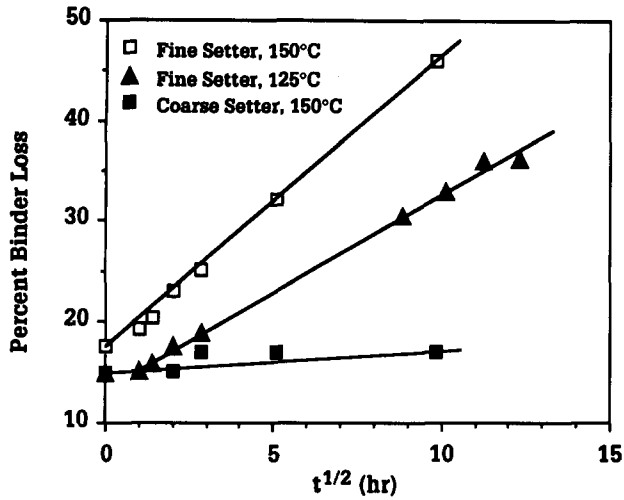
Fig. 10. Weight loss data from isothermal burnout experiments on MOR bars.

ticle size did not influence the weight loss in Stage II of this setter type (see Fig. 7).

The $t^{1/2}$ time dependence as observed for wicking in fine setter (Fig. 10) is similar to that observed for cast formation in slip casting or filtration processes.[32,33] Similar time dependence has also been observed in other debinding (by wicking) studies of injection-molded ceramic and metal powder compacts.[18,19,34] Conceptually, wicking is similar to the casting (or filtration) process when one considers that the setter bed (like the plaster mold) provides the suction force to pull the liquid from the part. It is shown in the following section that this mechanism of binder removal has strongly influenced the cracking pattern observed in large cross-section components.

As the temperature is increased, binder loss by evaporation becomes significant. Stage III of the binder removal process (Fig. 7) is defined in this paper as the region where vaporization dominated the binder loss process. In fine setter, a transition from Stage II to Stage III is expected as binder vaporization from the part surface becomes significant with increasing temperature at >150°C. In coarse setter, however, rapid weight loss by vaporization could start only at >250°C, when the protective cake (that formed in Stage II and acting as a barrier for further weight loss by wicking) breaks down due to decomposition of binder.

Binder loss by vaporization and/or decomposition in the absence of a setter bed has been considered in several recent publications. Barone & Ulicny[13] highlighted the earlier[12] experimental observation which showed that a uniform binder distribution was maintained during the majority of the burnout process in test specimens containing wax and polyethylene binder. Similar uniformity in binder distribution up to 40% weight loss was reported by Cima et al.[17] in their experiments with tape cast ceramics. These observations led to the

conclusion that capillarity-driven liquid migration from the interior to the part surface, followed by volatilization from the surface, was the dominant binder removal mechanism in these systems. This is similar to the process of drying of solvents from porous bodies. Barone & Ulicny[13] also indicated in their analysis that binder decomposition to lower molecular weight components further aided liquid migration due to lowered viscosities. Diffusion-controlled gas-phase transport appeared to become significant at the late stage of the drying-like binder removal process when surface vaporization rate could not be maintained by the liquid binder migration from the bulk. The diffusion control processes were also dominant when thermoset binders were used, i.e. when no liquid was present.[17,35]

Experimental determination of the binder distribution was carried out in the present study for AGT 100 rotors. Figure 11 summarizes the measured binder concentration gradients ΔC_1 (% binder loss from bulk — % binder loss from blade) and ΔC_2 (% binder loss from bulk — % binder loss from rotor hub surface) as a function of percentage total binder loss from the rotor for both fine and coarse setter. The rotors were obtained from interrupted burnout runs. Each data point represents an average of at least two TGA measurements on cored samples (approximately 12–40 mg) from a specific rotor area.
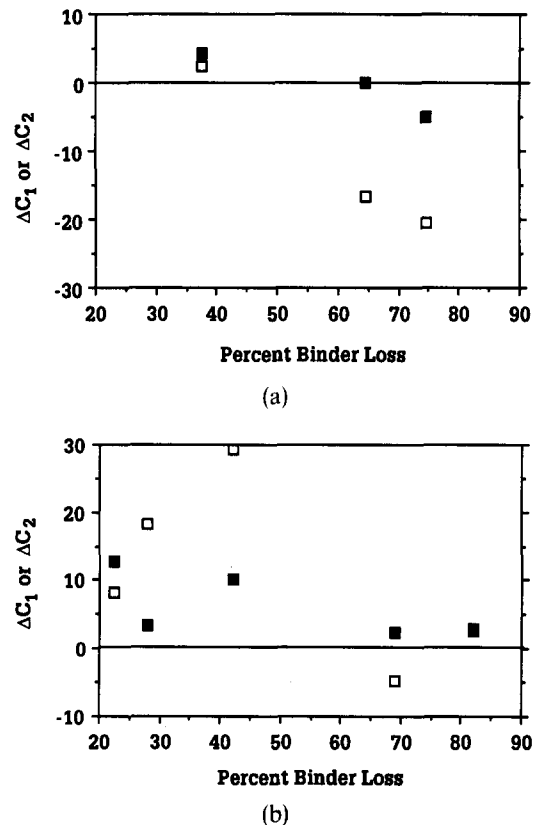

(a)

(b)

Fig. 11. Binder gradient formation in AGT 100 rotors. □, ΔC_1 is defined as (% binder loss from bulk — % binder loss from blade) and ■, ΔC_2 is defined as (% binder loss from bulk — % binder loss from rotor hub surface). (a) Fine setter; (b) coarse setter.

It is interesting to note that binder-rich blades and hub surface (compared to the bulk) were formed in the early stages of binder removal (<50% binder loss); the effect was particularly pronounced for the coarse setter in which, as mentioned earlier, a thick cake was formed which prevented binder migration away from the part surface. As the burnout progressed, a drying of the blades and hub surface (compared to the bulk) occurred in fine setter at 65% or higher total binder loss from the part. In coarse setter, however, drying of thin sections (blades) or the hub surface did not appear to occur even when as much as 80% binder was lost from the part.

The binder distribution data presented above are in general agreement with the observations from the weight loss rate data presented in Fig. 9. For example, in fine setter, at approximately 40–65% weight loss, a horizontal region similar to the constant rate drying was observed; this was followed by a falling rate period at >65% binder loss. The falling rate region in the later part of the burnout cycle represented the stage at which the supply of binder from the bulk was not sufficient to keep up with the vaporization rate from the surface. Under this condition (at 65% or higher weight loss for fine setter), a surface drying is expected and has been observed (Fig. 11) in AGT 100 rotors. The data from the coarse setter, on the other hand, show (in Fig. 9) that, even at 80% weight loss, the falling rate region did not start; this confirms the experimental observation (Fig. 11) that binder uniformity was maintained in coarse setter through this weight loss stage.

The lack of drying of binder in the part surface through a significant part of the burnout cycle, as shown in Fig. 11, is similar to those reported earlier.[12,17] The results indicate that capillarity-driven liquid migration from the bulk to the surface dominated the binder distribution process. The setter powder, however, strongly influenced the temperature at which vaporization (Stage III) started at the part surface. For example, in coarse setter, the temperature at which the majority of the binder was removed was substantially higher (Fig. 7) than that observed for fine setter. As a result, it is believed that the liquid removal was aided by the lower viscosity of the migrating binder, and thus surface drying was delayed substantially in coarse setter as compared to that observed in fine setter bed.

3.2 Cracking

Cracking problems related to binder removal are largely responsible for preventing injection molding from becoming a significant shape fabrication process specifically for large cross-section ceramic components. To compound this difficulty, information on the extent, nature and mechanisms of cracking

in injection-molded parts is very limited;[14,21-23,25] the data on cracking in large cross-section complex components containing thin and thick sections are virtually nonexistent. The results presented in this section represent the first attempt to describe the effects of some key burnout variables such as the setter types and thermal cycles on cracking, specifically in large silicon nitride components such as the AGT 100 rotors.

Both small and large cross-section parts were examined for cracks by X-ray radiography and sectioning after burnout and after sintering. In normal 10°C/h heating rate with fine or coarse setter, cracks did not form in MOR bars ($V/S = 0.15$ cm, where V is the part volume and S is the surface area); the spheres with $V/S = 0.37$ cm generally showed visually observable but small internal cracks, whereas AGT 100 rotors with an estimated V/S ratio of 0.54 cm (without the blades) exhibited major internal and surface connected cracks. Since injection-molded parts showed little dimensional shrinkage after binder burnout, despite the loss of a large volume of binder, the binder volume must be replaced by the formation of interconnected porosity or cracks. It appears that for small cross-section and small volume parts such as the MOR bars the pore volume that needs accommodation is sufficiently small, and thus cracks did not form in these parts. However, in spheres and AGT 100 rotors, the binder volume could not be accommodated by pore formation alone, thus cracks formed. The discussion in the remaining part of this section is limited to observations from AGT 100 rotors only.

Despite significant differences in the binder removal mechanisms in fine and coarse setter, the cracking patterns in rotors from both setter types at normal 10°C/h heating rate were approximately similar (Fig. 12). This figure shows a typical sintered rotor cross-section characterized by circumferential internal cracking parallel to the part surface with few or no surface connected radial cracks. The cracking pattern, however, changed drastically when the wicking process was substantially encouraged by subjecting the rotors in fine setters to a very slow cycle (e.g. 2°C/h) or a long hold (24 h or more) at 150°C. On sintering of these components, the parts showed the presence of a large crack in the midsection (Fig. 13). In addition, these parts also exhibited a strong tendency to external cracking, particularly in the form of radial cracks extending to the part surface (Fig. 13). Similar slow cycles or long hold at 150°C in coarse setter did not change the cracking pattern from that observed in normal 10°C/h runs (Fig. 12). The results confirm the earlier observations[20] that burnout cracks could not be eliminated simply by slowing down the heating rate.

No attempt has been made in this paper to analyze

Fig. 13. Cracking pattern in sintered AGT 100 rotors when wicking was the major contributor to the binder loss.
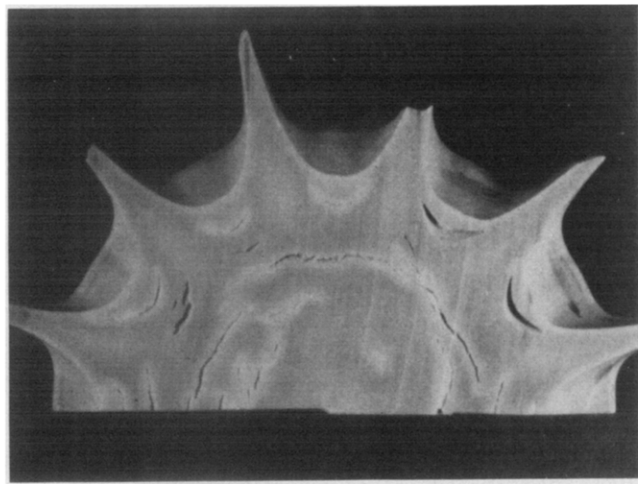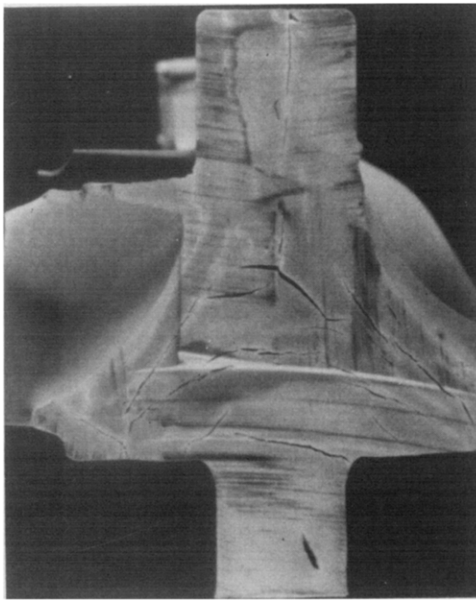
Fig. 12. Cracking pattern in AGT 100 rotors when coarse setter and/or rapid heating were used during burnout.

the changes in cracking pattern as described; evidently many variables are involved in the process. It should be emphasized, however, that wicking-induced particle rearrangement must be a key factor in cracking, since enhanced wicking caused a significant change in the cracking pattern. A possible mechanism of particle rearrangement as a result of setter powder-driven wicking is as follows. The wicking forces due to the setter can exert a significant drag on particles, as is observed in casting or filtration processes where migration of fine particles in the direction of the liquid flow is known to cause a significant porosity gradient.[36,37] Such migration of fines to the surface is unlikely in highly loaded injection-molded compacts. However, as a result of the liquid flow and external drag in the wicking environment, particle compaction is expected to start from the part surface, as shown schematically in Fig. 14. This type of particle rearrangement would prevent burnout shrinkage, as has been observed experimentally, and would result
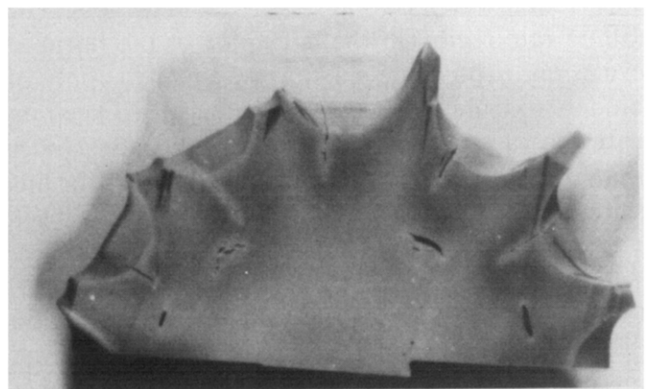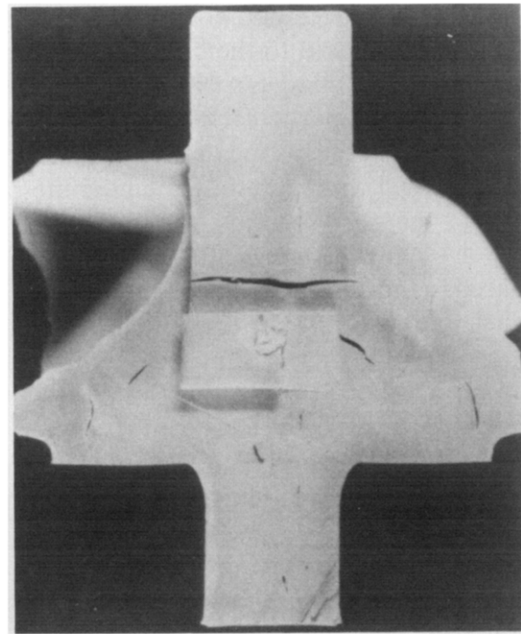
in internal cracking. Any nonuniformity in shrinkage in the part surface as a result of complex geometry and/or early surface drying would cause surface connected cracks similar to those formed in conventional drying processes.[38]

The results presented here indicate some significant and fundamental cracking difficulties in the fabrication of injection-molded large cross-section components using conventional thermoplastic-type binder systems. Several options have been considered to eliminate or minimize the burnout-related cracking. For example, NGK insulators[5] pursued joining of injection-molded air-foil sections with isopressed hub material in order to avoid the difficulties related to large cross-section parts. Other approaches include[39] use of coarser starting powder (to reduce capillary forces inside the part) and low wicking setter environment (to promote higher temperature binder removal) to eliminate formation of surface connected cracks in burnout, followed by use of compressive stresses (e.g. cold isostatic pressing and sintering or hot isostatic pressing) to eliminate internal defects. Other solutions would
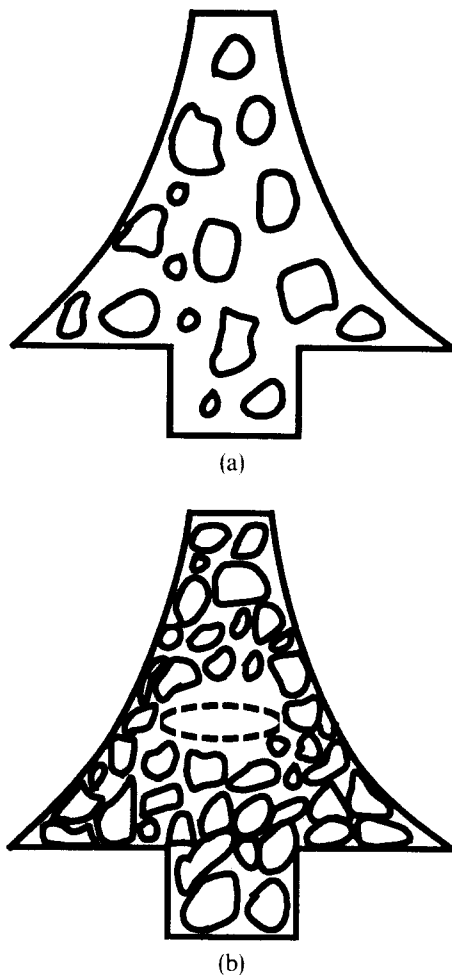
(a)

(b)

Fig. 14. Schematic description of internal crack formation in a wicking environment. (a) In the as-molded state, particles are all separated by binder; (b) particle compaction at the surface due to wicking-induced external drag resulting in internal crack.

most likely come from innovative use of binders and process conditions that would allow part shrinkage or eliminate the need for shrinkage after forming.

4 Summary and Conclusions

Injection molding of silicon nitride with a wax-based thermoplastic binder system has been critically evaluated with the goal of understanding the binder removal process and its impact on crack formation in large cross-section (>1 cm) components. Binder loss studies were performed in an inert environment on small and simple shapes such as MOR bars and spheres, as well as on large complex shapes such as a radial turbine rotor embedded in a setter powder. The setter powder bed provided part support and also acted as a wick during binder burnout and removed liquid binder from the part.

Binder loss was described in terms of three mechanisms: initial loss due to volume expansion of binder on melting and thermal expansion of binder, wicking of liquid binder due to capillary pull from the setter bed, and binder volatilization. The wicking was dominant when high surface area 'fine' setter

bed was used. It is proposed that wicking created a casting-like process in which the setter bed (similar to a plaster mold) provided the suction force to pull liquid from the part. When a low surface area 'coarse' setter powder bed was used, the wicking was prevented; as a result, volatilization from the part surface, similar to the drying of liquid from a porous bed, dominated the weight loss.

The parts showed little shrinkage in burnout, indicating that the binder volume must be replaced by the formation of interconnected porosity and/or cracks. In small cross-section (<1 cm) parts with small volume to surface ratio (e.g. MOR bars), the binder volume can easily be accommodated as pores without formation of cracks. Thus burnout cracking was not a concern for MOR bars, but major internal and surface connected cracks were formed in large parts such as the radial turbine rotors. Cracking in rotors could not be eliminated by variations of the wicking and volatilization environment through changes of the setter bed and thermal cycles; however, enhanced wicking in fine setters through slowing down of thermal cycles or long hold at 150°C significantly changed the cracking pattern. The results indicate that wicking induced external drag and the resulting particle rearrangement prevented parts shrinkage; thus it played an important role in component cracking. These results and the cracking behavior indicated some significant and fundamental difficulties in fabrication of injection-molded large cross-section components using thermoplastic-type binder systems. While these difficulties have been avoided successfully in recent component fabrication activities by innovative means, further improvement is expected to come from new and novel binder systems and processes that would allow uniform part shrinkage or eliminate the need for shrinkage after forming.

References

1. Mutsuddy, B. C., Injection molding research paves way to ceramic engine parts. *J. Ind. Res. Dev.*, **25** (1983) 76–80.

2. Edirisinghe, M. H. & Evans, J. R. G., Review: fabrication of engineering ceramics by injection moulding. I. Materials selection. *Int. J. High Technology Ceramics*, **2** (1986) 1–31.
3. Edirisinghe, M. H. & Evans, J. R. G., Review: fabrication of engineering ceramics by injection moulding. II. Techniques. *Int. J. High Technology Ceramics*, **2** (1986) 249–78.
4. Ohnsorg, R., TenEyck, M. & Sweeting, T., Development of injection molded rotors for gas turbine applications. ASME Paper No. 86-GT-45 presented at the International Gas Turbine Conference, Düsseldorf, West Germany, 8–12 June 1986.
5. Kaneno, M. & Oda, I., Sintered silicon nitride turbocharger rotor. SAE Paper No. 940013 presented at the International Congress and Exposition, Detroit, Michigan, 27 February–2 March 1984, p. 3.
6. Greim, J., Hunold, K., Schwetz, K. A. & Lipp, A., Injection molded sintered turbocharger rotors: a comparison of SSiC with SSN and SRBSN. In *Proc. Third Int. Symp. on Ceramic Materials and Components for Engines*, ed. V. J. Tennery. The American Ceramic Society, Inc., Westerville, OH, 1989, pp. 1365–75.
7. Bandyopadhyay, G., Mahoney, F. M., Sordelet, D. J. & French, K., Fabrication and evaluation of silicon nitride heat engine components. In *Proc. Third Symp. on Ceramic Materials and Components for Engines*, ed. V. J. Tennery. The American Ceramic Society, Inc., Westerville, OH, 1989, pp. 1397–406.
8. Miyachi, J. & Kobayashi, Y., Development of silicon nitride turbine rotors. SAE Paper No. 950313 presented at the International Congress and Exposition, Detroit, Michigan, 25 February–1 March 1985.
9. Helms, H. E., Heitman, P. W., Lindgren, L. C. & Thrasher, S. R., *Ceramic Applications in Turbine Engines*. Noyes Publications, Park Ridge, NJ, 1986, pp. 83–106.
10. Helms, H. E., AGT 100 project summary. ASME Paper No. 88-GT-223 presented at the Gas Turbine and Aeroengine Congress, Amsterdam, The Netherlands, 6–9 June 1988.
11. Bandyopadhyay, G., French, K. W., Sordelet, D. J. & Moergenthaler, K. D., Fabrication and development of axial silicon nitride gas turbine rotors. *J. Eng. Gas Turbines and Power*, **113** (1991) 643–9.
12. Barone, M. R., Ulicny, J. C., Hengst, R. R. & Pollinger, J. R., Removal of organic binders in ceramic powder compacts. In *Ceramic Transactions, Vol. 1A, Ceramic Powder Science II*, ed. G. L. Messing, E. R. Fuller Jr & H. Hausner. American Ceramic Society, Inc., Westerville, OH, 1988, pp. 575–83.
13. Barone, M. R. & Ulicny, J. C., Liquid-phase transport during removal of organic binders in injection-molded ceramics. *J. Am. Ceram. Soc.*, **73** (1990) 3323–33.
14. German, R. M., *Powder Injection Molding*. Metal Powder Industries Federation, Princeton, NJ, 1990.
15. German, R. M., Theory of thermal debinding. *Int. J. Powder Metallurgy*, **23** (1987) 237–45.
16. Wright, J. K., Evans, J. R. G. & Edirisinghe, M. J., Degradation of polyolefin blends used for ceramic injection molding. *J. Am. Ceram. Soc.*, **72** (1989) 1822–8.
17. Cima, M. J., Lewis, J. A. & Devoe, A. D., Binder distribution in ceramic greenware during thermolysis. *J. Am. Ceram. Soc.*, **72** (1989) 1192–9.
18. Bao, Y. & Evans, J. R. G., Kinetics of capillary extraction of organic vehicle from ceramic bodies. Part I. Flow in porous media. *J. Eur. Ceram. Soc.*, **8** (1991) 81–93.
19. Bao, Y. & Evans, J. R. G., Kinetics of capillary extraction of organic vehicle from ceramic bodies. Part II. Partitioning between porous media. *J. Eur. Ceram. Soc.*, **8** (1991) 95–105.
20. Quackenbush, C. L., French, K. & Neil, J. T., Fabrication of

21. Wright, J. K., Edirisinghe, M. J., Zhang, J. G. & Evans, J. R. G., Particle packing in ceramic injection molding. *J. Am. Ceram. Soc.*, **73** (1990) 2653–8.
22. Zhang, J. G., Edirisinghe, M. J. & Evans, J. R. G., A catalogue of ceramic injection moulding defects and their causes. *Industrial Ceramics*, **9** (1989) 72–82.
23. Evans, J. R. G. & Edirisinghe, M. J., Interfacial factors affecting the incidence of defects in ceramic mouldings. *J. Mater. Sci.*, **26** (1991) 2081–8.
24. French, K. W., Neil, J. T. & Turnbaugh, L. T., Composition for injection molding. US Patent 4456713, 1984.
25. Bandyopadhyay, G. & French, K., Fabrication of near-net-shape silicon nitride parts for engine application. *J. Eng. Gas Turbines and Power*, **108** (1986) 536–9.
26. Pasto, A. E., Neil, J. T. & Quackenbush, C. L., Microstructural effects influencing strength of silicon nitride. In *Proc. of Int. Conf. on Ultrastruct. Proc. of Ceram. and Composites*, ed. L. L. Heath and D. R. Ulrich. John Wiley & Sons, New York, 1984, pp. 476–89.
27. Farris, R. J., Prediction of the viscosity of the multimodal suspensions from unimodal viscosity data. *Trans. Soc. Rheology*, **12** (1968) 281–301.
28. Mangels, J. A. & Williams, R. M., Injection molding ceramics to high green densities. *Bull. Am. Ceram. Soc.*, **62** (1983) 601–6.
29. Mutsuddy, B. C. & Kahn, L. R., A practical approach in relating capillary viscosity and spiral-length data for molding ceramic mixes. In *Forming of Ceramics*, ed. J. A. Mangels & G. L. Messing. American Ceramic Society, Inc., Westerville, OH, 1984, pp. 251–8.
30. Zhang, J. G., Edirisinghe, M. J. & Evans, J. R. G., The use of modulated pressure in ceramic injection moulding. *J. Eur. Ceram. Soc.*, **5** (1989) 63–72.
31. Koenigsberg, W. D. & Neil, J. T., Ceramic binder removal studies using projection radiography. In *Nondestructive Testing of High Performance Ceramics*, ed. A. Varz & J. Snyder. American Ceramic Society, Inc., Westerville, OH, 1987, pp. 539–46.
32. Adcock, D. S. & McDowall, I. C., Mechanism of filter pressing and slip casting. *J. Am. Ceram. Soc.*, **40** (1957) 355–62.
33. Fennelly, T. J. & Reed, J. S., Mechanics of pressure slip casting. *J. Am. Ceram. Soc.*, **55** (1972) 264–8.
34. Lograsso, B. K. & German, R. M., Thermal debinding of injection molded powder compacts. *Int. J. Powder Metallurgy*, **22** (1990) 17–22.
35. Lewis, J. A. & Cima, M. J., Direct observation of binder distribution process in 2-D porous networks during thermolysis. In *Ceramic Transactions, Vol. 12, Ceramic Powder Science III*, ed. G. L. Messing, S. Hirano & H. Hausner. American Ceramic Society, Inc., Westerville, OH, 1990, pp. 583–90.
36. Shirato, M., Sanbuichi, M., Kato, H. & Aragaki, T., Internal flow mechanisms in filter cakes. *AIChE Journal*, **15** (1969) 405–9.
37. Tiller, F. M. & Cooper, H., The role of porosity in filtration: Part V. Porosity variation in filter cakes. *AIChE Journal*, **8** (1962) 445–9.
38. Cooper, A. R., Quantitative theory of cracking and warping during the drying of clay bodies. In *Ceramic Processing Before Firing*, ed. G. Y. Onoda Jr & L. L. Hench. John Wiley & Sons, Inc., New York, 1978, pp. 261–76.
39. Bandyopadhyay, G., French, K. W., Bowen, L. J. & Neil, J. T., Method for fabricating large cross-section injection molded ceramic shapes. US Patent 4708838, 1987.

sinterable silicon nitride by injection molding. *Ceram. Eng. Sci. Proc.*, **3** (1982) 20–34.